Three-Dimensional Simulations of Classical Novae

A. Kercek[1], W. Hillebrandt[1], and J. W. Truran[2]

[1] Max-Planck-Institut für Astrophysik, Karl-Schwarzschild-Strasse 1, D-85740 Garching, Germany
[2] Laboratory for Astrophysics and Space Research, Enrico Fermi Institute, University of Chicago, Chicago, IL 60637, USA

Abstract. We present first results of three-dimensional (3D-) calculations of turbulent and degenerate hydrogen-burning on top of a C+O white dwarf of 1.0 $M_\odot$. The simulations are carried out by means of a code which solves Euler's equation for an arbitrary equation of state together with a nuclear reaction network and the energy input from nuclear reactions on a Cartesian grid covering a fraction of the white dwarf's surface and accreted envelope. The flow patterns we obtain are very different from those of earlier 2D simulations using the same initial conditions and the same numerical resolution. The possibility of self-enrichment of the accreted hydrogen-rich envelope with carbon and oxygen from the surface layers of the white dwarf during the violent phase of the burning is investigated, and it is demonstrated that self-enrichment proceeds too slowly if the accreted gas has near-solar CNO-abundances at the onset of the thermonuclear runaway. As a result, we do not find a fast nova outburst. This conclusion remains valid if the initial metallicity of the accreted gas is raised by a factor of five. Therefore we conclude that fast nova outbursts indeed require huge enrichments of C and O, as postulated from spherically symmetric models, and that the mechanism which leads to such enhancements must operate prior to the outburst.

Key words: Stars: novae, cataclysmic variables - white dwarfs; Physical data and processes: convection - hydrodynamics - nuclear reactions, nucleosynthesis, abundances

1. Introduction

The standard model for the outburst of a classical nova is a thermonuclear runaway (TNR) in the accreted hydrogen-rich envelope on top of a white dwarf in a close binary system (Starrfield 1989, 1993, 1995; Truran 1982, 1990). Spherically symmetric models of the runaway, based on realistic nuclear reaction rate networks and mixing-length theory (MLT) of convection, have been investigated by many authors (Starrfield et al. 1974, 1985; Prialnik et al. 1978; Mac Donald 1980), and the results were in good agreement with observational data, such as the total amount of energy released and the metallicity and the abundances of the expelled envelope material, provided considerable enrichment of the envelope with CNO-elements was assumed. Although the actual numbers depend on the mass of the white dwarf and the accretion rate, typical enhancements of up to a factor of 10 relative to solar values were required for models of fast novae.

Despite of the success of these models, two questions remain to be answered:

- 1. Where does the enrichment come from?
- 2. What is changed if one avoids the mixing-length theory of convection?

In this paper we concentrate on the second question and will eliminate one suggested answer to the first one in passing. We shall mainly follow the arguments given in a recent work by us (Kercek et al. 1998; henceforth referred to as KHT), where these questions were addressed by direct two-dimensional simulations. For convenience we first summarize here the numerical method as well as the main results obtained in KHT.

In KHT (as well as here) we performed numerical simulations based upon the hydro-code PROMETHEUS (Fryxell et al. 1989), a PPM-type code with nuclear reactions included. Curvature effects were ignored and the surface layers of the white dwarf as well as its envelope were represented by a plane-parallel sheet. The advantage of this approach was that periodic boundary conditions could be used, thereby avoiding common problems of numerical simulations of free convection, namely that reflecting boundaries may act like a containment and may affect the flow patterns in an unphysical way. Effects coming from the finite numerical resolution were investigated and it was found that, as far as the general properties of the simulations were concerned, a grid of moderate resolution. e.g. 220 × 100 (horizontal × vertical) grid points, covering a total of 1800km × 1000km of the white dwarf's surface and envelope, was sufficient to obtain stable results for integral quantities such as the energy generation rate and the rate of mixing of carbon and oxygen from the white dwarf into the envelope.

In our version of PROMETHEUS, nuclear reactions are incorporated by solving together with the hydrodynamics a nuclear reaction network including 12 nuclear species, i.e., ^{1}H, ^{4}He, ^{12}C, ^{13}C, ^{13}N, ^{14}N, ^{15}N, ^{14}O, ^{15}O, ^{16}O, ^{17}O, and ^{17}F, linked by reactions described in Wallace & Woosley (1981). The reaction rates are taken from Thielemann (private communication). Following Müller (1986), we solve the network equations and the energy source equation simultaneously to avoid numerical instabilities.

Since the accretion process prior to the TNR needs several 10^5 years in order to get an initial model for the multi-dimensional simulations, one has to calculate the accretion phase and the slow stages of the burning by means of one-dimensional implicit hydro codes. Here as well as in KHT we used a model computed to the onset of the vehement phase of the TNR by Glasner et al. (1997). During this early phase, hydrogen-rich matter of solar composition (Z = 0.015) is accreted onto the surface of a 1 $M_\odot$ C+O white dwarf at an accretion rate of $5.0 \cdot 10^{-9} M_\odot yr^{-1}$. As the temperature rises at the bottom of the envelope convection sets in. Convection is taken into account by the MLT in the one dimensional model. The model provides the density, temperature, entropy, and composition profiles at the point at which the temperature at the bottom of the envelope reaches 10^8 K. The mass of the hydrogen shell is then about $2 \cdot 10^{-5} M_\odot$ and the metallicity is now Z = 0.02. This model was mapped onto a radial row of the 2D grid in KHT, relaxed for several hundred dynamical time scales, and then mapped onto the full 2D grid. In the present work, the same procedure is applied to a 3D grid. Finally, an initial perturbation is superimposed upon this hydrostatic configuration.

The main features of the 2D flow fields which showed up in KHT were the appearance of small persistent coherent structures of very high vorticity (and velocity) compared to the background flow. Although they were not fully resolved they caused effects that were essentially independent of the resolution. During the early phase of the thermonuclear runaway they dominated the flow patterns and resulted in very little overshoot and mixing. At late times, after steady slow mixing and with increasing nuclear energy production, they became weak, but showed up again after hydrogen had mainly been burnt and the energy generation rate dropped. The net effect was that KHT did find some self-enrichment, but on time-scales much longer than in previous calculations. Moreover, for initially solar composition of the accreted gas the rise time of the temperature was very long, of the order of 1000s, and peak temperatures never exceeded $2 \cdot 10^8$K. Therefore these models did not resemble the properties of a fast nova.

We mention in passing that similar 2D simulations have been carried out by Glasner et al. (1997) although with rather different results. In particular they found that strong overshoot and mixing lead to high metal enrichments in the envelope yielding a fast nova. The possible origin of this discrepancy was addressed in KHT.

Of course, the question arises if these conclusions would remain valid if the assumption of 2D symmetry were dropped. First, one does not expect to find the small-scale stable vortices in 3D because they are a property of plane-parallel 2D flows, as was discussed in KHT. On the other hand, one also expects the dominant linear scale of convective eddies to be smaller in 3D than in 2D and, therefore, mixing and convective overshooting could be even less efficient than was found by KHT.

In the following sections we will answer this question. In Sect. 2 we briefly describe the parameters of the models we have computed. In Sect. 3 we present and discuss the results of two sets of computations, one with solar initial composition of the accreted gas and a second with 5 times higher metal abundances. Some conclusions and an outlook follow in Sect. 4. We will concentrate on the astrophysical aspects of our simulations and leave results and questions related to the physics of turbulent combustion in the so-called well stirred regime to a forthcoming paper.

2. The models

The computational grid of our present computations covers a fraction of 1000km (vertical) × 1800km × 1800km (lateral) of the white dwarf's surface and envelope by 100 × 220 × 220 grid points in a Cartesian mesh. This is equivalent to the "low resolution" case of KHT. The lateral grid is equidistant whereas in vertical direction we use a non-equidistant grid with the highest spatial resolution (5km) in the white dwarf's surface and the bottom layers of its envelope. As an initial perturbation we increase the temperature by 1% in 20 zones right on top of the white dwarf. In contrast to KHT, we choose a somewhat larger perturbed area in order to save computer time. This, however, is not a problem since the initial conditions are a bit artificial anyhow, and we saw in our previous 2D simulations that information about the initial perturbation is lost after about 15s.

Since we fix the initial conditions according to the model of Glasner et al. (1997) the only parameter which still can be varied within reasonable limits is the initial metallicity of the envelope. But, because solving the reactive Euler-equations in 3D with realistic equations of state is "expensive" (on 512 processors of a CRAY T3E one time-step needs about 8s CPU-time, and about 2×10^5 time-steps are required per simulation), we cannot perform an extensive parameter study. We decided rather to choose solar composition for a first simulation (in order to compare the results with our earlier 2D computations) and to increase the metallicity to 10% in a second run. This second simulation is meant to investigate whether or no moderately higher CNO abundances lead to significantly more violent nuclear burning, thereby changing a "slow" nova to a fast one. Although it is certainly of interest to increase C and O by another factor of 2 to 3 in order to match the conditions which would give a fast nova in 1D simulations, we did not do it because of obvious inconsistencies of our initial model in that case.

Combustion in novae is peculiar because convective overturn times are much shorter than the nuclear reaction time-scale. Therefore, in general, stirring proceeds much faster then nuclear burning. In our approach to this problem, namely by direct numerical simulations, we resolve the large scale inhomogeneities and velocity fluctuations well, but the small scale dissipation and mixing is dominated by numerical discretization effects. This is not a problem as far as the energy transport by convective motions is concerned because the energy flux is predominantly carried by the largest eddies. Mixing by turbulent motions, however, happens on very small scales which are definitely not resolved in our computations. Therefore we will overestimate the mixing due to the numerical diffusion of matter on the grid scale. But since, as we shall show, even with our treatment mixing is too slow for a fast nova to occur, direct simulations are a conservative approach to the problem under consideration here.

3. Results of the 3D simulations

3.1. The case of near-solar metallicity (Z=0.02)

In this subsection we present and discuss the results we have obtained for an envelope of nearly solar metallicity, the main emphasis being on a comparison with KHT. The initial abundances were obtained by evolving the accreted envelope of a given metallicity through steady hydrogen burning to the vehement stage of the TNR. We shall first analyse the evolution of the convective flow fields, and then discuss integral quantities such as the laterally averaged temperature and the nuclear composition. We computed this model over about 400s.

3.1.1. The evolution of the flow fields

In order to visualize our results we present them in the form of 2-dimensional cuts and iso-surfaces in three dimensions. The 2D-cuts show, colour-coded, the absolute values of the velocity as a function of time. They indicate where in the envelope of the white dwarf most of the convective transport is happening and can easily be compared with our earlier 2D results. In contrast, the iso-surfaces of the absolute values of the velocity field at fixed times are used to discuss the characteristic structure and scales of the convective eddies.

Figure 1 gives the temporal evolution of the velocities for a typical 2D cut. As in the 2D simulations of KHT, the surface layer is ignited by an "ignition string" perpendicular to the plane shown. After a couple of seconds the entire surface layer is burning and the first convective eddies form. This stage is reached a little earlier than in the 2D simulations, mainly because a larger volume was perturbed initially. From then on the evolution is very different from the 2D case. No regular structures appear. In contrast, the flow field is very irregular. Violent eruptions occur occasionally at later times, followed by periods of rather quiet burning. Towards the end of the computations, convective motions extend all the way into the upper envelope.

The evolution of the convective patterns can be seen more clearly in the iso-surface plots Figs. 2 to 4. Figure 2, taken at 50s, shows that most of the fast eddies in the beginning are confined to a narrow layer near to the white dwarf's surface, extending over roughly 150km. This burning layer is well separated from an upper convective zone with large but slow eddies. But even the convective motions near the surface are slow in comparison to the sound velocity which is above 10^8cm/s there. During this phase, the burning matter does not expand significantly and also the upper envelope is only moderately heated from below. Consequently, the temperature rises in the burning region above 10^8K, and the burning becomes more violent. As is shown in Fig. 3, after about 100s, convective velocities begin to exceed 10^7cm/s and some eddies start to penetrate into the upper envelope. From then on very efficient heat transport by convection leads to an expansion of the envelope, and energy going into lift-off, and adiabatic energy losses balance essentially gains from nuclear burning. After 200s, finally, the entire envelope is well stirred by convective eddies of all sizes with typical velocities around $6{\cdot}10^6$cm/s (see Fig. 4). It is obvious that the flow fields in 3D are very different from the ones in 2D, as computed in KHT, and one expects that this will also effect integral quantities.

When we stopped this set of computations after 400s, the nuclear energy generation rate is approximately constant throughout the white dwarf's envelope and a stage of nearly steady hydrogen burning is reached. The average nuclear energy generation rate has come down to a few times 10^{13}erg/g/s, missing the conditions for a fast nova by far. The total energy released by nuclear reactions is $5.8{\cdot}10^{44}$erg which should be compared with the value of $2.1{\cdot}10^{45}$erg for our 2D simulation at the same time.

3.1.2. Temperature evolution, energy generation and convective mixing

The temperature evolution of this near-solar metallicity model is depicted in Figs. 5 and 6, and the corresponding energy generation rates are given in Fig. 7.

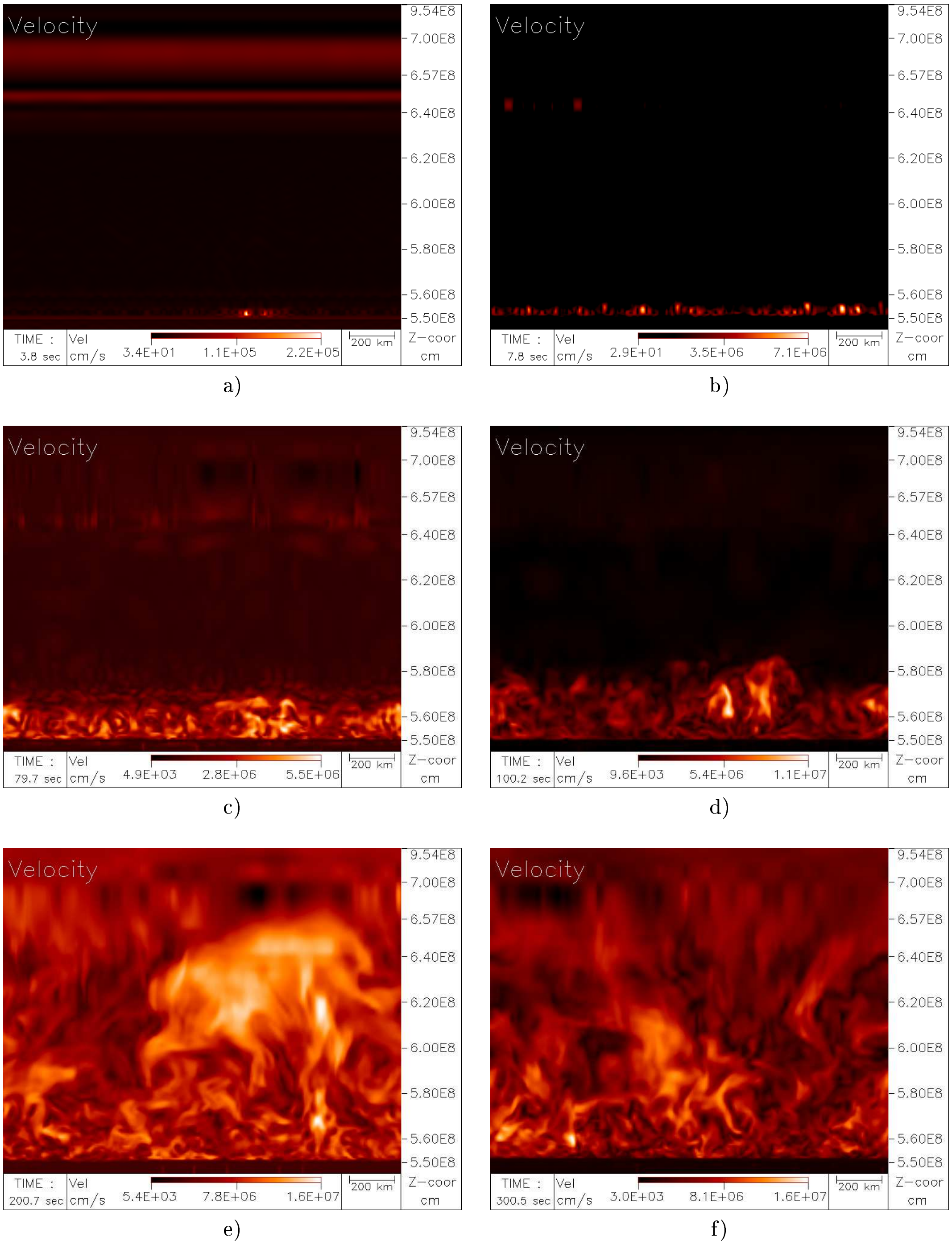

Fig. 1. Snapshots of the velocity field of the three-dimensional run with an initial metallicity of Z = 0.02. Shown are vertical slices through the calculation domain. The absolute values of the velocity at each point are color coded. Note that the "radial" coordinate is logarithmic above 6500 km.

In Fig. 5 we picked the temperature of the hottest zone and plotted it as a function of time. The first short drop reflects the ignition phase. The following rapid rise to the peak value of about $1.1{\cdot}10^8$K is due to degenerate nuclear burning without efficient convective energy transport and expansion, as was discussed in the previous subsection. This phase is followed by some expansion and adiabatic cooling, accompanied by the onset of more efficient convective energy transport and mixing. Consequently, the maximum temperature rises again, but now its peak value is found a bit further out in the envelope. These temperatures are typically 10 to 20 % below what we have obtained in our 2D simulations mainly because, as we shall

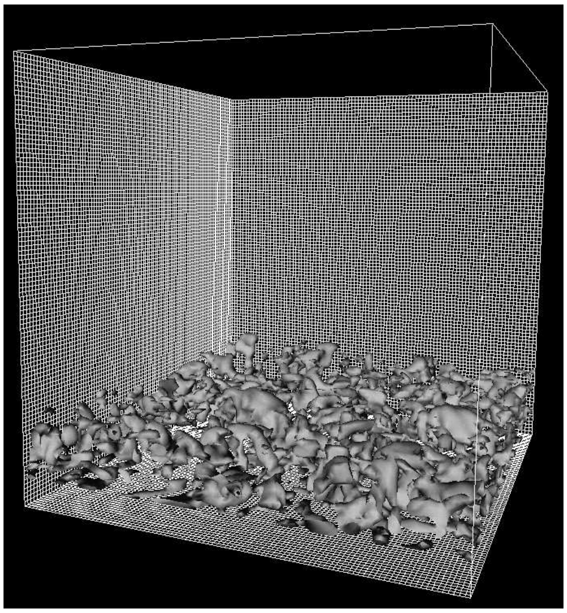

Iso-surface $v = 1.5 \cdot 10^6$ cm/s

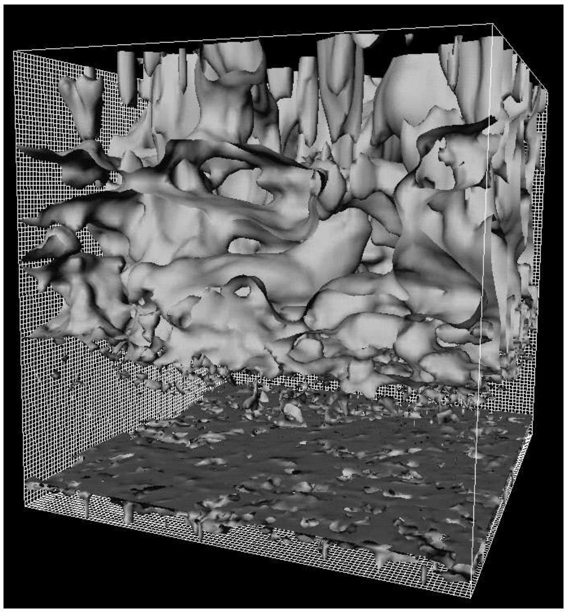

Iso-surface $v = 1.0 \cdot 10^5$ cm/s

Fig. 2. Iso-surfaces of the absolute value of the velocity for the 3D simulation with an initial metallicity of Z = 0.02 at t = **50 seconds**. The (800km)^3 cube shown in this figure is only a fraction of the total computational domain. Two distinctly different convective layers can be seen: one of high velocity near to the surface of the white dwarf, and a second one of low velocities in the outer envelope.

see, mixing of fresh C and O from the white dwarf into the hydrogen-rich envelope is slower in 3D than in 2D.

Figure 6 shows snapshots of the temperature distribution, averaged over horizontal planes. With the exception of a clear spike at 98s, indicating nuclear burning in a well confined surface layer, the distributions are very smooth, reflecting the nearly adiabatic average temperature gradient of a fully convective stratified envelope.

These effects are more clearly seen in the vertical profiles of the nuclear energy generation rate, again averaged over horizontal planes, given in Fig. 7. For the first about 100s we observe a rapid increase of the energy generation rate in the layers just on top of the white dwarf, and convective energy transport is insufficient to induce fast burning in the outer parts. Towards the end of this simulations one can see that a stage of nearly steady burning is reached throughout most of the envelope.

Finally, in Figs. 8 and 9 we show the mass fraction of ^{12}C and the total metallicity for the same snapshots as in the previous figures. The sharp discontinuity at $5.5 \cdot 18^8$cm in the initial values presents the white dwarf's surface. The initial mass fraction of ^{12}C is about 0.06 % only because steady hydrogen burning prior to the TNR has transfered most of the originally solar CNO isotopes into ^{14}N, whereas the metallicity is untouched. One can see in Fig. 8 as well as in Fig. 9 that fresh ^{12}C is mixed into the envelope by convective undershoot at a very moderate rate only. By the time the electron degeneracy is largely removed (after about 100s) mixing has just doubled the metallicity in most of the burning zones. This is the main reason why we did not obtain a violent outburst.

3.1.3. Mass loss and nucleosynthesis

In concluding this section, we want to discuss briefly possible observable consequences of this model. Peak outflow velocities are reached after 170s and they amount to $5 \cdot 10^6$cm/s at a radius of 6400km which is far below the escape velocity from the white dwarf of about $6 \cdot 10^8$cm/s (see Fig. 10). Typically, the velocities are also a factor of two below those we obtained in the 2D run at the same instants of time. Therefore, although we are loosing mass from our computational grid by outflow (see Fig. 11), there is no direct mass ejection from the white dwarf. In contrast, mass loss will happen in form of a wind from the outer envelope which was not included in our computations.

Conclusions concerning the chemical composition of the wind, therefore, are rather uncertain. Nevertheless we can obtain rough estimates by looking at the abundances we find in the computational domain. As can be seen in Figs. 12 through 14, after about 400s (in reality already after 200s) the composition of freshly synthesized (radioactive) isotopes is homogeneously distributed throughout the white dwarf's envelope. Since we expect that fast convective mixing will proceed all the way out to optically thin regions one can also expect that this composition is a fair representation of the matter which is lost from the

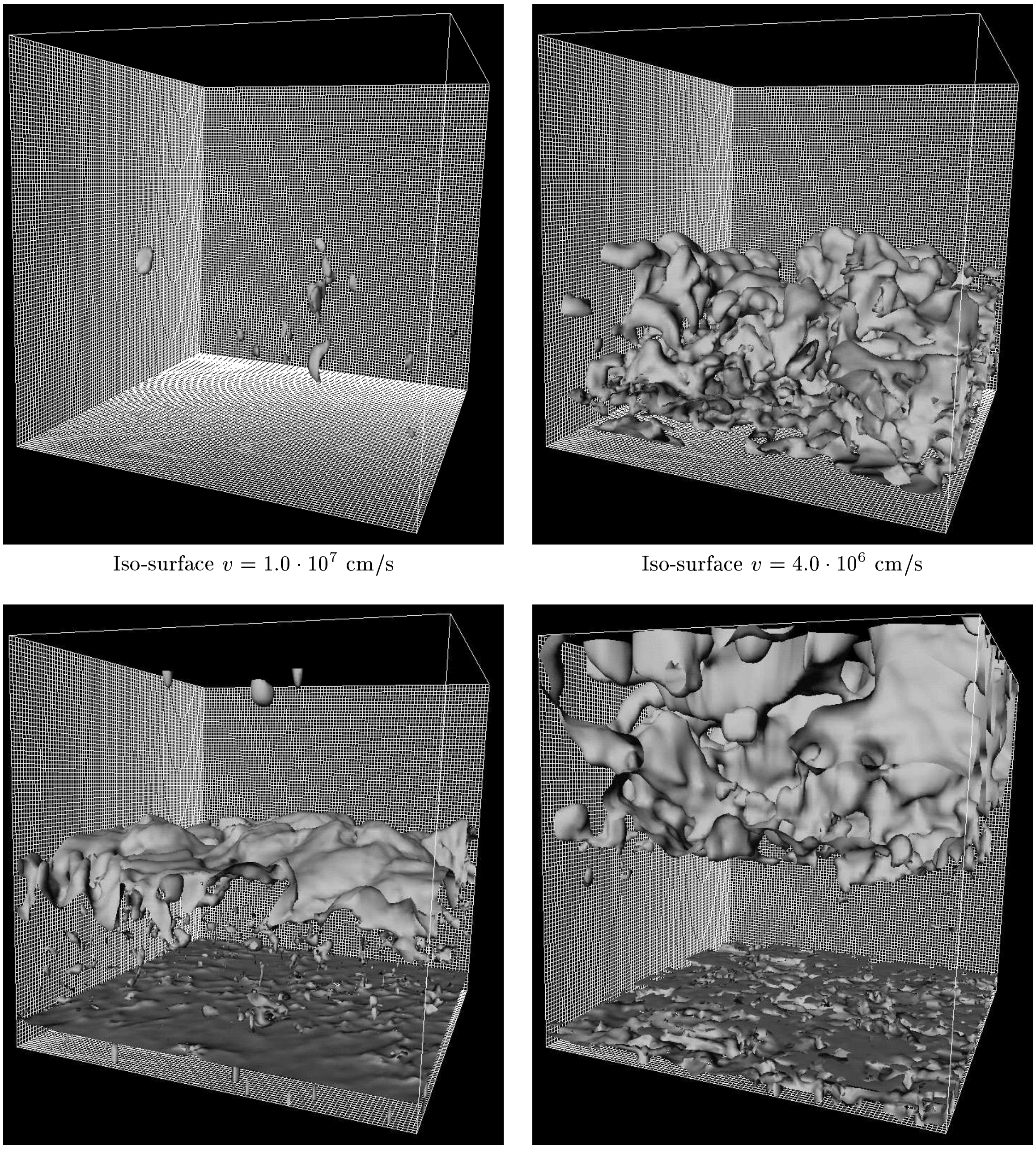

Iso-surface $v = 1.0 \cdot 10^7$ cm/s

Iso-surface $v = 4.0 \cdot 10^6$ cm/s

Iso-surface $v = 8.0 \cdot 10^5$ cm/s

Iso-surface $v = 2.0 \cdot 10^5$ cm/s

Fig. 3. Same as Fig.2, but at $t = \mathbf{100}$ **seconds**. It can be seen that typical convective velocities still decrease with increasing distance from the white dwarf's surface, but the different layers begin to mix. Those close to the surface are heavily stirred by nuclear energy generation.

white dwarf ejected in the wind. At late times, radioactive decay heating by these isotopes dominates the energy production in all but the innermost layers of the envelope, but the overall enrichment of CNO isotopes is only moderate, probably not more than a factor of five to six relative to the initial values.

3.2. A model with Z=0.1

In one-dimensional nova simulations initial metal abundances largely in excess of their solar values are required to drive a fast outburst. Since we have demonstrated that self-enrichment of the envelope by convective undershoot and dredge-up of matter from the white dwarf does not happen during the outburst, we decided to run a model in which the envelope was already enriched from the start.

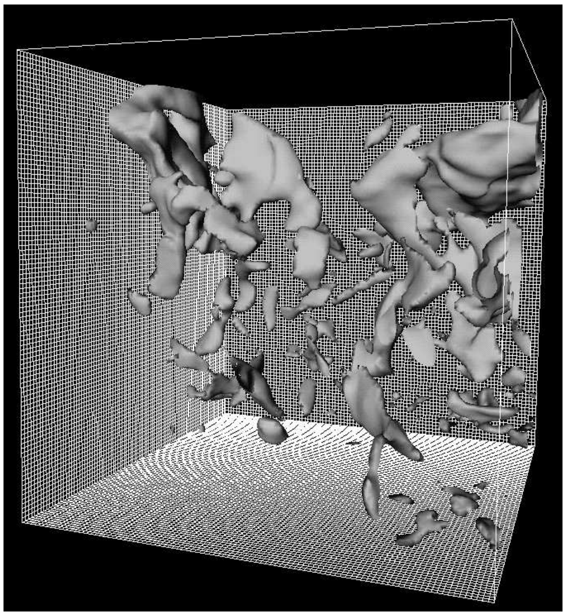

Iso-surface $v = 1.0 \cdot 10^7$ cm/s

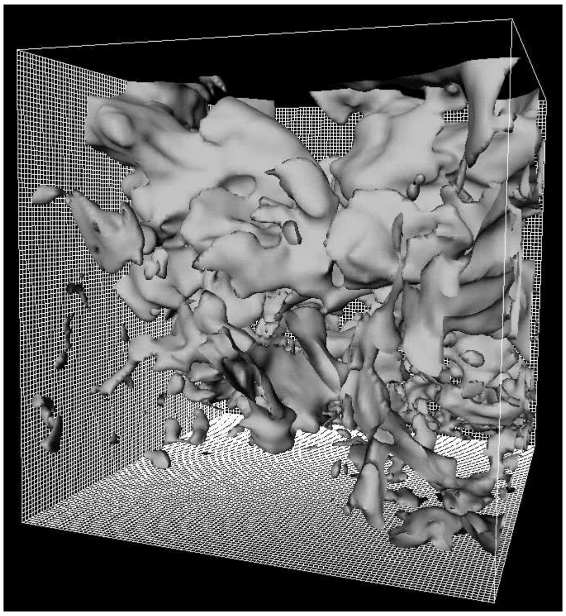

Iso-surface $v = 8.0 \cdot 10^6$ cm/s

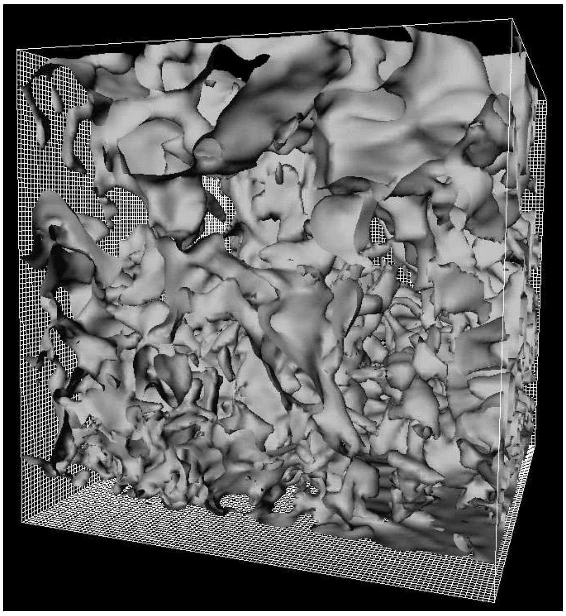

Iso-surface $v = 4.0 \cdot 10^6$ cm/s

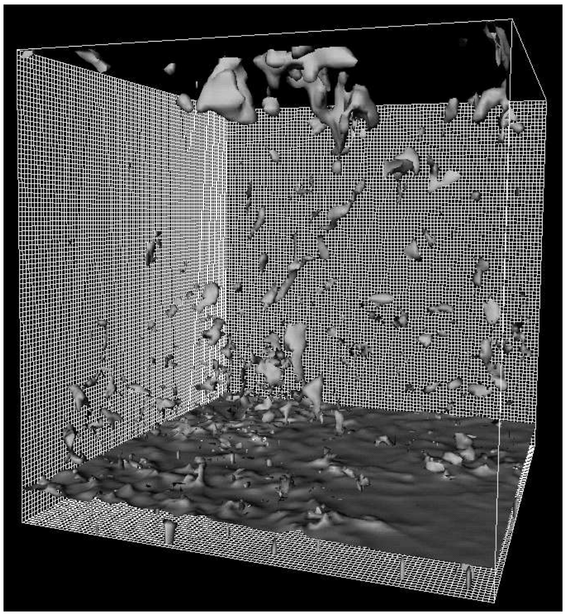

Iso-surface $v = 1.0 \cdot 10^6$ cm/s

Fig. 4. Same as Fig.2, but at $t = \mathbf{200}$ **seconds**. The convective eddies no longer show a clear structure. The entire computational domain is well stirred and covered by eddies of all sizes and different velocities.

In order to avoid large inconsistencies (this model was not evolved in the same way as the low-metallicity one), we increased Z to 0.1 only and constructed a new equilibrium model which had the same temperature structure as before. Burning was then ignited by raising the temperature by 1% in 20 zones of the bottom layer of the accreted envelope, and all other properties of the model were identical to the previous one. Of course, an enrichment by a factor of five is still below what is commonly assumed in 1D simulations but one might hope for more violent burning and, therefore, also faster mixing of C and O already in this case, if convective motions are treated properly. However, as we shall demonstrate, this is not the case. We find that the evolution proceeds considerably faster than in the low-metallicity case, but the final outcome is not too different in both cases.

The flow patterns look very similar to those shown in Fig. 1, with the exception that already after about 80s

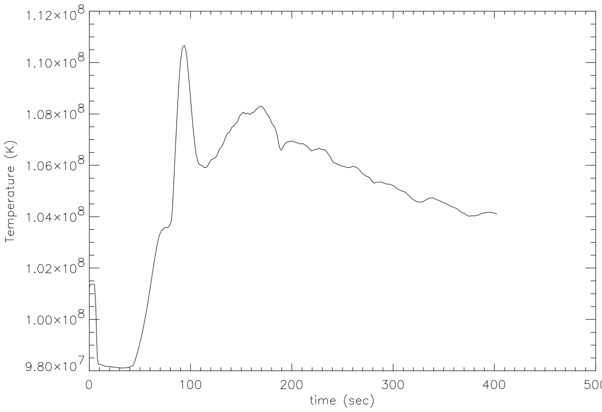

Fig. 5. Time evolution of the horizontally averaged temperature in the hottest layer of the envelope for the 3D run with Z = 0.02.

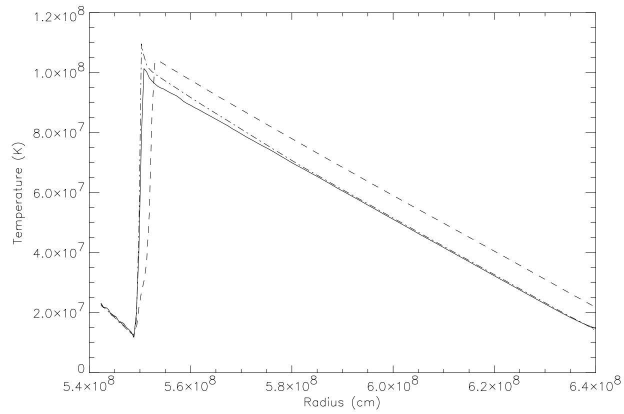

Fig. 6. Horizontally averaged vertical temperature profiles for the 3D run with Z = 0.02 at 0 s (solid line), 98 s (dashed-dotted line), and 400 s (dashed line), respectively.

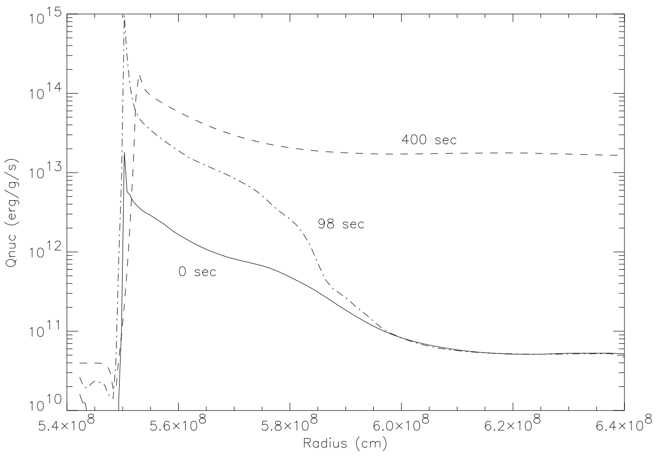

Fig. 7. Same as Fig. 5, but for the horizontally averaged vertical profile of the energy generation rate.

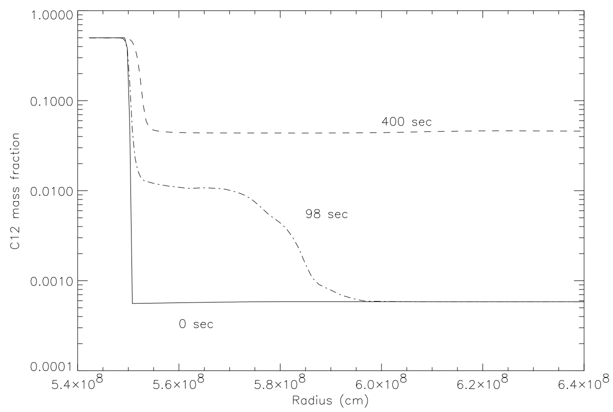

Fig. 8. Same as Fig. 6, but for the horizontally averaged vertical profiles of the ^{12}C mass fraction.

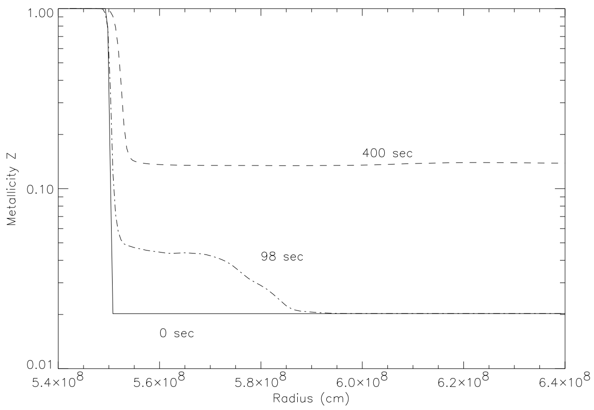

Fig. 9. Same as Fig. 6, but for the horizontally averaged vertical profiles of the metallicity.

velocities above 10^7cm/s are observed, and after about 150s peak velocities reach $2{\cdot}10^7$cm/s, nearly a factor of 2 higher than in the low-metallicity run. The second effect is that peak temperatures are now a bit higher (see Figs. 15 and 16, to be compared with Figs. 5 and 6), and also the energy generation rate exceeds the previous one, but not by much. After 160s a state of burning is reached which is nearly indistinguishable from the low-metallicity case at 400 seconds. Even the metallicity in the envelope (Fig. 17) is only moderately higher than before.

We therefore conclude that, although originally higher CNO-abundances speed up the thermonuclear burning, going to 5 times solar metallicity is still insufficient for a fast nova. The reason seems to be that, despite the fact that the consumption of hydrogen is faster in the beginning, the time scale for the temperature rise is still too long, i.e. on the order of 100s. This, in turn, means that, as before, the envelope begins to expand and cool once the temperature exceeds 10^8K, much too low for a fast nova. Very fast mixing of white dwarf material into the envelope during the early phase of the TNR could, in principle,

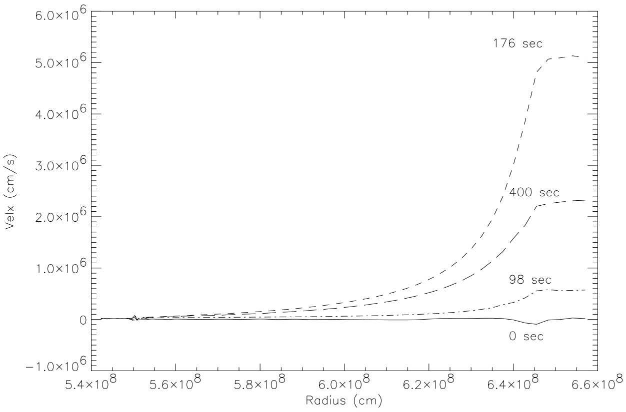

Fig. 10. Horizontally averaged vertical profiles of the vertical component of the velocity at four different times for the 3D simulation with Z = 0.02.

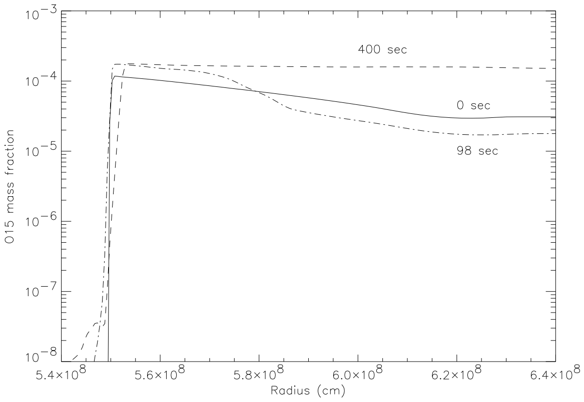

Fig. 12. Snapshots of the horizontally averaged vertical profiles of the ^{15}O mass fraction for the case Z = 0.02.

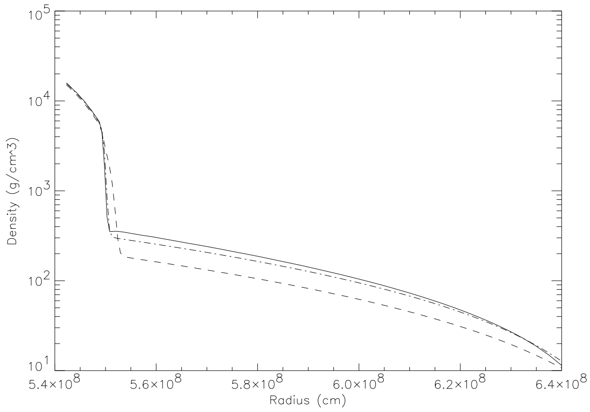

Fig. 11. Horizontally averaged vertical profiles of the density for the run with Z = 0.02 (0 s solid line, 200 s dashed-dotted line, 400 s dashed line, respectively).

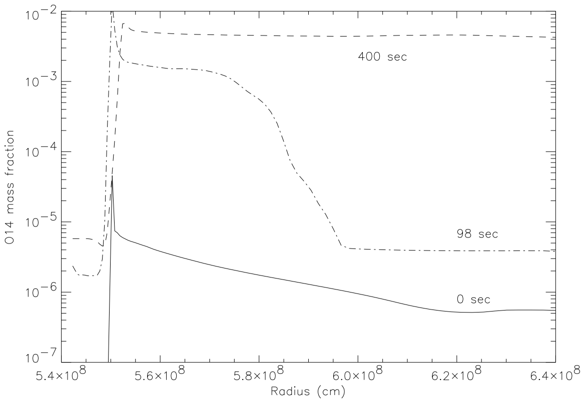

Fig. 13. Same as Fig. 12, but for the ^{14}O mass fraction.

overcome this problem but we do not find such a mixing. In contrast, the 3D simulations mix even less than the 2D models of KHT.

4. Summary and conclusions

We have presented the first 3-dimensional simulations of thermonuclear models of classical novae. We have shown that the results differ, in several aspects, considerably from those of previous 2-dimensional simulations and we conclude that this and similar problems have to be carried out in 3D in order to give reliable results. The main reason is that the flow fields in 3D are very different from those in 2D and, therefore, all quantities which depend on them, such as convective energy transport and mixing, will also differ in both cases. For example, in 3D we find, not unexpectedly, more power in small scale motions than in our previous 2D simulations which leads to less convective undershoot into the white dwarf's surface and consequently less dredge-up of C and O. This, in turn, makes explosive hydrogen burning less violent, weakening the chances for getting a fast nova that way.

Therefore we arrive at the conclusion that self-enrichment of the accreted envelope with C and O during the outburst is very unlikely, if not impossible, and our simulations rule out one of the suggestions for changing a slow nova into a fast one. A more likely solution to this problem seems to be large enrichment prior to the outburst by either shear-induced instabilities at the interface between the white dwarf and its envelope (like in an accretion belt) or some kind of diffusive or convective mixing during the long quiet accretion phase.

Finally, we want to point out that the type of numerical simulations we have performed leave room for improvements. Firstly, as was mentioned already in the introduction, in our numerical method mixing on small scales is due to numerical diffusion. It is difficult to estimate quantitatively its effect. It appears to be safer to include mixing by small scale turbulence explicitly by a subgrid model, as was done for the propagation of nuclear flames

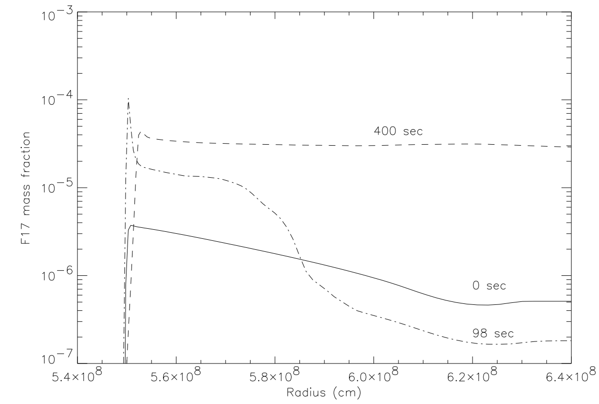

Fig. 14. Same as Fig. 12, but for the ^{17}F mass fraction.

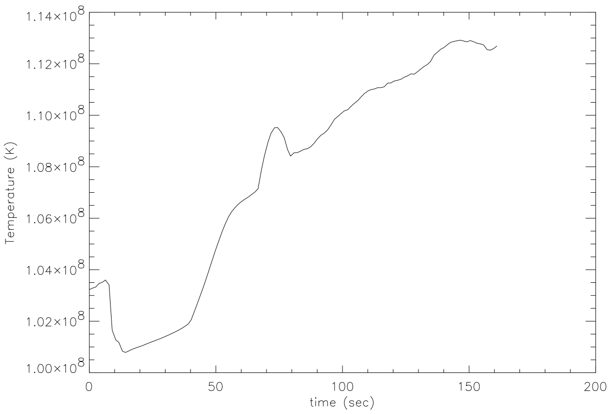

Fig. 15. Temperature in the hottest shell of the envelope for the 3D run with an initial metallicity of Z = 0.1.

by Niemeyer & Hillebrandt (1995). Secondly, the kind of problems we have tackled here with brute force, namely a problem in which the typical velocities are far below the sound velocity, should be better approached by means of (nearly incompressible) implicit hydrodynamics schemes which are presently being developed. It is obvious that one would like to explore a larger fraction of the parameter space, but this can only be done with more efficient codes.

Acknowledgments. The authors are grateful for many enlightening discussions with Stanford E. Woosley, Jens C. Niemeyer and Hans Ritter. They thank Ami Glasner and Eli Livne for supplying the initial model, Ewald Müller for an earlier version of the PROMETHEUS code, and Rudi Fischer and Jakob Pichlmeier for their help in preparing a parallel version of the code. They also thank the staff members of the Rechenzentrum Garching for their support during the computations. This work was supported in part by NASA under Grant NAG 5-3076, by DOE under contract No. B341495 at the University of Chicago, and by the Deutsche Forschungsgemeinschaft under Grant Hi 534/3-1. The computations were performed at the Rechenzentrum Garching on a Cray T3E.

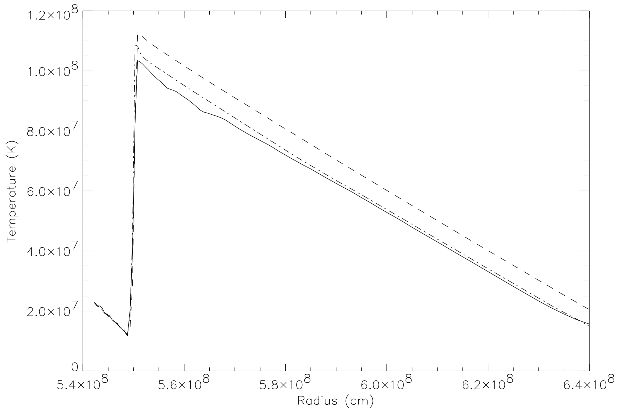

Fig. 16. Snapshots of the horizontally averaged vertical profiles of the temperature for the run with Z = 0.1 initially, at 0 s (solid line), 78 s (dashed-dotted line) and 160 s (dashed line).

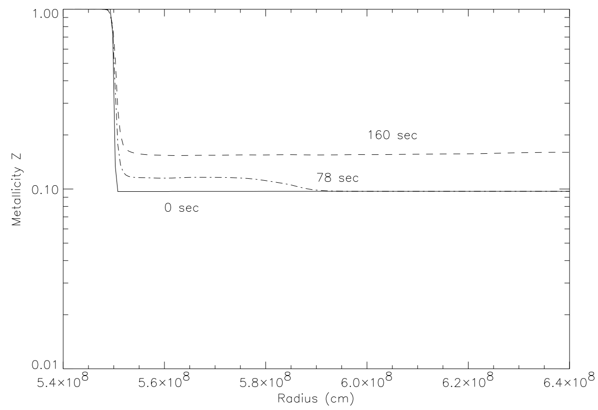

Fig. 17. Same as Fig. 16, but for the metallicity.

References

Fryxell B.A., Müller E., Arnett W.D., 1989, Max-Planck-Institut für Astrophysik Report 449, Garching, Germany

Glasner S.A., Livne E., Truran J.W., 1997, ApJ 475, 754

Kercek A., Hillebrandt W., Truran, J.W., 1998, A&A 337, 379

Mac Donald J., 1980, MNRAS 191, 933

Müller E., 1986, A&A 162, 103

Niemeyer J.C., Hillebrandt W., 1995, ApJ 452, 779

Prialnik D., Shara M.M., Shaviv G., 1978, A&A 62, 339

Starrfield S., 1989, in *The Classical Novae*, ed. M. Bode and A. Evans, (Wiley: NY), 39

Starrfield S., 1993, in *The Realm of Interacting Binary Stars*, ed. J. Sahade, G.E. McCluskey, and Y. Kondo (Dordrecht: Kluwer), 209

Starrfield S., 1995, in *Physical Processes in Astrophysics*, ed. I. Roxburgh, and J.L. Masnou, (Springer: Heidelberg), 99

Starrfield S., Sparks W.M., Truran J.W., 1974, ApJ Suppl. 28, 247

Starrfield S., Sparks W.M., Truran J.W., 1985, ApJ 291, 136

Truran J.W., 1982, in *Essays in Nuclear Physics*, ed. C.A. Barnes, D.D. Clayton and D.N. Schramm (Cambridge: Cambridge U. Press), 467

Truran J.W., 1990, in *The Physics of Classical Novae*, ed. A. Cassatella and R. Viotti, (Heidelberg: Springer), 373

Wallace, R.K., and Woosley, S.E., 1981, ApJS, 45, 389